

Thermodynamic investigation of the magnetic phase transitions of CaMnO_3 and SrRuO_3

J.J. Neumeier,^{1,2} A.L. Cornelius,³ and K. Andres²

¹*Department of Physics, Florida Atlantic University, Boca Raton, Florida 33431*

²*Walther-Meissner-Institut, Walther-Meissner-Strasse 8, D-85748 Garching, Germany*

³*Department of Physics, University of Nevada Las Vegas, Las Vegas, Nevada, 89154-4002*

(Received 10 November 2000; revised manuscript received 5 July 2001; published 5 October 2001)

Measurements of the linear thermal expansion $\Delta l/l$ and molar heat capacity C_p at constant pressure are presented on antiferromagnetic CaMnO_3 and ferromagnetic SrRuO_3 in the neighborhood of their magnetic phase transitions. The jumps in the linear thermal-expansion coefficient α and C_p are used to calculate the influence of pressure on the magnetic ordering temperatures T_c through the Ehrenfest relation. Good agreement is obtained with measured values of dT_c/dP .

DOI: 10.1103/PhysRevB.64.172406

PACS number(s): 75.40.Cx, 75.50.Ee, 75.50.Cc, 65.40.-b

Second-order phase transitions are typically characterized according to a scheme due to Ehrenfest.¹ The lowest-order derivative of the Gibbs function's G that shows a discontinuity at the phase transition gives the order of the transition. For example, in the case of a second-order phase transition, the thermodynamic variables volume $V=(\partial G/\partial P)T$, and entropy $S=-(\partial G/\partial T)P$, are continuous at the phase transition. Their derivatives, which are the second derivatives of G , however, are discontinuous leading to the characterization as a second-order phase transition. The transition from normal to superconducting in zero magnetic field is considered to bear the closest resemblance to an ideal second-order phase transition. The Ehrenfest relation establishes a connection between the pressure derivative of the phase transition's critical temperature T_c , the jump in the volume thermal expansion coefficient β , $\Delta\beta$, and the jump in the molar heat capacity C_p , ΔC_p . It is given by

$$\frac{dT_c}{dP} = v T_c \frac{\Delta\beta}{\Delta C_p}, \quad (1)$$

where v is the molar volume. This relation also holds in anisotropic materials if the pressure P is replaced by uniaxial stress P_i in the i th crystallographic direction and $\Delta\beta$ is replaced by the thermal-expansion jump $\Delta\alpha_i$ in the same direction. In recent years the Ehrenfest relation has been employed in the study of high-quality single crystals of high temperature²⁻⁴ and organic⁵ superconductors to reveal the uniaxial pressure derivatives dT_c/dP_i for the transition temperature to the superconducting state T_c . Excellent agreement with directly measured values of dT_c/dP_i , as well as the hydrostatic pressure derivative dT_c/dP , have been obtained.

Similar studies in low-dimensional magnetic systems could be of interest to probe the existence of anisotropy in the magnetic interaction. However, the phase transition between paramagnetic and antiferromagnetic (or ferromagnetic) behavior often does not possess the character typical of an ideal second-order phase transition¹ in that it deviates slightly from the form expected for a second-order phase transition through a divergence above and below the transition. This arises because of magnetic anisotropy that increases the number of components associated with the mag-

netic order parameter.⁶ Typically, these type of phase transitions would be handled within the framework of the modern theory of critical phenomena. However, this theory does not at present possess a simple expression from which dT_c/dP_i values can be calculated. Following the guidelines of Ehrenfest,¹ if the volume and entropy remain continuous across the phase transition, Eq. (1) should remain valid. Recently, Eq. (1) was applied in the study of $\text{La}_{0.83}\text{Sr}_{0.17}\text{MnO}_3$, which is a ferromagnet belonging to a class known to exhibit an unusually large magnetoresistance.⁷ Good agreement was found with the pressure derivative of its Curie temperature. It appeared of value to investigate the application of Eq. (1) to other interesting magnetic systems, which is the objective of the present work. In this case we report on thermal expansion and heat capacity studies of polycrystalline CaMnO_3 , a well-known antiferromagnet, and find good agreement between the measured value of dT_c/dP and that calculated through Eq. (1). We also report on thermal-expansion measurements of the ferromagnet SrRuO_3 , which has the distinction of being the only transition-metal ferromagnet devoid of a 3d element. With the help of published heat-capacity data⁸ for ΔC_p we calculate dT_c/dP and also find good agreement with measured values. These results suggest that similar studies on single-crystalline low-dimensional magnetic systems would successfully yield the uniaxial pressure derivatives dT_c/dP_i .

The polycrystalline sample of CaMnO_3 was prepared from high-purity CaCO_3 and MnO_2 . Stoichiometric quantities were weighed and mixed with an agate mortar and pestle for 7 min followed by reaction for 20 h at 1100 °C. The specimen was reground for 5 min, reacted for 20 h at 1150 °C, reground for 5 min, reacted for 20 h at 1250 °C, reground for 5 min, reacted for 46 h at 1300 °C, reground for 5 min, pressed into pellets, reacted for 17 h at 1300 °C and cooled at 0.4 °C/min to 30 °C. Iodometric titration, to measure the average Mn valence, indicates the oxygen content falls within the range 3.00 ± 0.01 . The polycrystalline SrRuO_3 sample was prepared from high-purity SrCO_3 and RuO_2 powders in a similar manner and reacted at 1100 °C for 20 h. The specimen was reground for 8 min, reacted for 48 h at 1175 °C, reground for 8 min and reacted at 1250 °C for 20 h. Finally, the specimen was reground for 8 min,

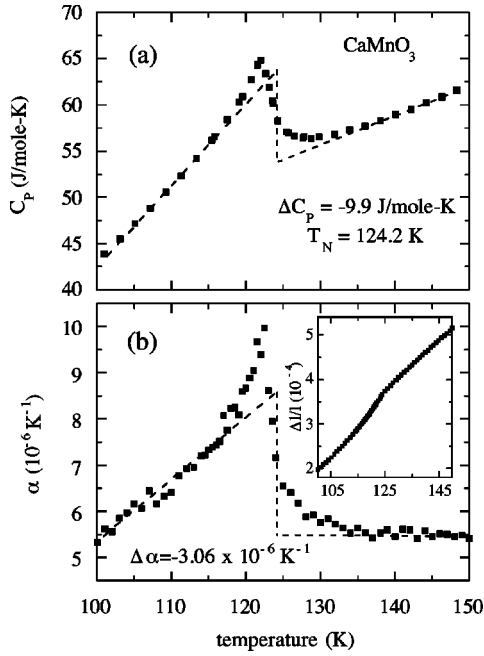


FIG. 1. (a) Molar heat capacity C_p is plotted versus temperature in the region near the antiferromagnetic phase transition for CaMnO_3 . The dashed lines indicate the extrapolations used to determine the jump in C_p at the phase transition ΔC_p . (b) The linear thermal expansion coefficient α is plotted versus temperature near the phase transition; the dashed lines depict the extrapolations used to determine the jump in α at the phase transition $\Delta\alpha$. In the inset the linear thermal expansion $\Delta l/l$ is plotted versus temperature in the region near the phase transition.

pressed into pellets, and reacted at 1280 °C for 20 h. Powder x-ray diffraction revealed no secondary phases in either specimen; this technique can detect such phases only if they are above the 2% level. Both specimens possess orthorhombic crystal structures. The linear thermal expansion was measured using a capacitive dilatometer constructed of high-purity quartz;⁹ the samples were warmed slowly through the magnetic transition at a rate less than 70 mK/min. It is assumed that the obtained thermal-expansion data represent an average over all crystallographic directions. The heat capacity was measured using a standard thermal relaxation technique.

The magnetic properties of the CaMnO_3 specimen were recently presented in another paper.¹⁰ Our measurements of the molar heat capacity near the magnetic ordering temperature are illustrated in Fig. 1(a) where C_p is plotted versus temperature T . Taking the C_p data, dividing by the temperature, and then integrating provides the entropy which is continuous (not shown). To determine the jump in C_p at the Néel temperature $T_c = 124.2$ K we draw two straight lines through the data above and below T_c as depicted by the dashed lines in the figure. The dashed lines indicate the form of an ideal second-order phase transition as describable within a mean-field theory. This method provides the value $\Delta C_p = -9.9 \pm 0.7$ J/mole-K for CaMnO_3 .

Linear thermal expansion $\Delta l/l$ is plotted versus temperature in the inset of Fig. 1(b). The measurements were con-

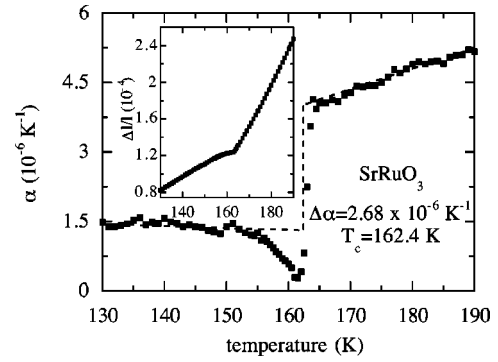


FIG. 2. The linear thermal expansion coefficient α is plotted versus temperature near the ferromagnetic transition temperature for SrRuO_3 . The dashed lines indicate the extrapolations used to determine the jump in α at the phase transition $\Delta\alpha$. In the inset the linear thermal expansion $\Delta l/l$ is shown in the same temperature region.

ducted on a 0.84 mm long polycrystalline specimen. The linear thermal expansion is continuous through the transition, as typical for a second-order phase transition. We note that a more detailed plot of $\Delta l/l$ near T_c (with temperature spacing of 0.02 K) also reveals a continuous transition. A point-by-point derivative of these data (spaced at either 0.5 K or 1 K) yielded the linear thermal-expansion coefficient α that is also plotted in Fig. 1(b). As with the heat-capacity data, straight lines are drawn through the data above and below T_c illustrating the form of an ideal second-order phase transition; for the heat capacity and thermal-expansion data the dashed lines are also consistent with an entropy-conserving construction often used in the analysis of phase transitions. A value of $\Delta\alpha = -3.06 \times 10^{-6} \pm 0.18 \times 10^{-6} \text{ K}^{-1}$ is obtained. The shape of both transitions differs from that observed in high-temperature superconductors^{2,3,11,12} in that both C_p and α diverge slightly as T_c is approached from below. The superconductors more closely approximate an ideal second-order phase transition, although anisotropies can lead to fluctuations and deviations from mean-field behavior.²¹ Although the shape of the transition in CaMnO_3 deviates from the idealized behavior, this is quite common. Most importantly, our measurements clearly reveal continuity in the volume through the phase transition and hence the second-order nature. The values for ΔC_p and $\Delta\beta = 3\Delta\alpha$ obtained from the data in Fig. 1 can now be used to calculate dT_c/dP with Eq. (1). The molar volume is calculated with the lattice parameter¹³ for the CaMnO_3 unit cell of 3.73 Å and $T_c = 124.2$ K. A value of $dT_c/dP = 3.60 \pm 0.51$ K/GPa is obtained which agrees, within experimental error, with the measured value¹⁴ of $dT_c/dP = 4.2 \pm 0.2$ K/GPa.

We now turn to our linear thermal expansion measurements of SrRuO_3 that are displayed in Fig. 2. In the inset the linear thermal expansion $\Delta l/l$ is displayed versus temperature in the region near the ferromagnetic Curie temperature T_c ; $\Delta l/l$ versus T is clearly continuous through the phase transition, this is also the case for a more detailed data set with temperature spacing of 0.02 K. A point-by-point derivative of the data yields the linear thermal expansion coefficient α . It is interesting to note that the obtained α curve

bears a close resemblance to that observed in ferromagnetic Invar alloys^{15,16} where α decreases significantly below T_c as a result of the ferromagnetic transition. As in Fig. 1, straight lines are drawn through the data to determine the jump in α at $T_c=162.4$ K, which is found to be $\Delta\alpha=2.68\times 10^{-6}\pm 0.22\times 10^{-6}$ K⁻¹; the dashed lines closely approximate an entropy-conserving construction. A small divergence in α is observed as the transition is approached from above or below, similar to that observed in CaMnO₃. We determine $\Delta C_P=-6.5\pm 0.5$ J/mole-K from published C_P data.⁸ Using these values of $\Delta\alpha$ and ΔC_P along with the lattice parameter¹⁷ of 3.92 Å our calculation using Eq. (1) yields $dT_c/dP=-7.28\pm 1.25$ K/G Pa which agrees well with measured values of dT_c/dP (-7.9 K/G Pa, -5.7 ± 0.2 K/G Pa, and -6.3 K/G Pa).¹⁷⁻¹⁹ We note that SrRuO₃ is known to exhibit a very large magnetic anisotropy.²⁰ It would be of interest to obtain the uniaxial pressure derivatives dT_c/dP_i through thermal expansion measurements of single crystals. If anisotropy were to exist among the dT_c/dP_i values, it might provide insight into the destruction of ferromagnetism observed to result as Ca is substituted for Sr in SrRuO₃.

The results presented above illustrate good agreement between measured values of dT_c/dP and those calculated us-

ing thermodynamic parameters and the Ehrenfest relation. In addition, these two systems illustrate thermodynamic transitions with both positive and negative dT_c/dP values. Our results indicate that the Ehrenfest relation yields reliable values for dT_c/dP in both antiferromagnetic CaMnO₃ and ferromagnetic SrRuO₃, although the method may have higher uncertainties than direct measurement due to the deviation in shape of the transitions from that expected for ideal second-order transitions and the manner in which one extrapolates near the transition to determine the jump. The results presented herein and our previous experiments⁷ suggest that the uniaxial pressure derivatives dT_c/dP_i in such systems can also be obtained through similar analysis. Such investigations would probe the existence of anisotropy in the magnetic exchange interaction.

We acknowledge valuable discussions with Michael Kund and Yi-Kuo Yu as well as financial support from NSF contract DMR-9982834 (J.J.N.), NATO contract CRG 970260 (J.J.N. and K.A.), the Bayerische Akademie der Wissenschaften (J.J.N. and K.A.), DOE/EPSCoR Contract No. DE-FG02-00ER45835 (A.L.C.), and DOE Cooperative Agreement Grant No. DE-FC08-98NV13410 (A.L.C.).

¹A.B. Pippard, *Elements of Classical Thermodynamics for Advanced Students of Physics* (Cambridge University Press, London, 1966), p. 136.

²C. Meingast, O. Krauf, T. Wolf, H. Wühl, A. Erb, and G. Müller-Vogt, *Phys. Rev. Lett.* **67**, 1634 (1991); C. Meingast, J. Karpinski, E. Jilek, and E. Kaldis, *Physica C* **209**, 591 (1993).

³M. Kund and K. Andres, *Physica C* **205**, 32 (1993).

⁴M. Kund, J.J. Neumeier, K. Andres, J. Markl, and G. Saemann-Ischenko, *Physica C* **296**, 173 (1998).

⁵M. Kund, H. Veith, H. Müller, K. Andres, and G. Saito, *Physica C* **221**, 119 (1994).

⁶R.M. White and T.H. Geballe, *Long Range Order in Solids* (Academic Press, New York, 1979), p. 17.

⁷J.J. Neumeier, K. Andres, and K.J. McClellan, *Phys. Rev. B* **59**, 1701 (1999).

⁸P.B. Allen, H. Berger, O. Chauvet, L. Forro, T. Jarlborg, A. Junod, B. Revaz, and G. Santi, *Phys. Rev. B* **53**, 4393 (1996).

⁹M. Kund, *Uniaxiale Effekte in Organischen und Keramischen Supraleitern* (Harri Deutsch, Reihe Physik, Frankfurt am Main, 1995), ISBN 3-8171-1468-0.

¹⁰J.J. Neumeier and J.L. Cohn, *Phys. Rev. B* **61**, 14 319 (2000).

¹¹F. Gugenberger, C. Meingast, G. Roth, K. Grube, V. Breit, T. Weber, H. Wühl, S. Uchida, and Y. Nakamura, *Phys. Rev. B* **49**,

13 137 (1994).

¹²R.A. Fisher, J.E. Gordon, and N.E. Phillips, *J. Supercond.* **1**, 231 (1988).

¹³E.O. Wollan and W.C. Koehler, *Phys. Rev.* **100**, 545 (1955).

¹⁴J.A. Kafalas, N. Mnyk, K. Dwight, and J.M. Longo, *J. Appl. Phys.* **42**, 1497 (1971).

¹⁵E.F. Wasserman, *Ferromagnetic Materials*, edited by K.H.J. Buschow and E.P. Wohlfarth (Elsevier, Amsterdam, 1990), Vol. 5, p. 238.

¹⁶T. Kiyama, K. Yoshimura, K. Kosuge, Y. Ikeda, and Y. Bando, *Phys. Rev. B* **54**, 756 (1996).

¹⁷M. Shikano, T.-K. Huang, Y. Inaguma, M. Itoh, and T. Nakamura, *Solid State Commun.* **90**, 115 (1994).

¹⁸J.J. Neumeier, A.L. Cornelius, and J.S. Schilling, *Physica B* **198**, 324 (1994).

¹⁹N. Menyuk, J.A. Kafalas, K. Dwight, and J.B. Goodenough, *J. Appl. Phys.* **40**, 1324 (1969).

²⁰A. Kanbayasi, *J. Phys. Soc. Jpn.* **41**, 1876 (1976).

²¹V. Pasler, P. Schweiss, C. Meingast, B. Obst, H. Wühl, A.I. Rykov, and S. Tajima, *Phys. Rev. Lett.* **81**, 1094 (1998); C. Meingast, V. Pasler, P. Nagel, A. Rykov, S. Tajima, and P. Ols-son, *ibid.* **86**, 1606 (2001).